Electrical Antenna Downtilt in UMTS Network

Tero Isotalo, Jarno Niemelä, and Jukka Lempiäinen

Institute of Communications Engineering, Tampere University of Technology
P.O.BOX 553, FIN-33101 TAMPERE, FINLAND
email: {tero.isotalo, jarno.niemela, jukka.lempiainen}@tut.fi

Abstract: **In this paper, the impact of the base station electrical antenna downtilt on UMTS network performance is studied. The effect of the base station antenna height, vertical beamwidth, and site spacing on the optimum electrical downtilt angle has been evaluated in a macrocellular environment. Both downlink and uplink performances are considered with a special attention to soft handover areas. The results are based on system-level simulations utilizing a Monte-Carlo approach. According to the results, the base station antenna vertical beamwidth has the greatest impact on the optimum downtilt angle. A wider antenna vertical beamwidth requires a larger downtilt angle in order to obtain the optimum system performance. In addition, compared to antenna vertical beamwidth, site spacing and base station antenna height affect optimum downtilt angle in a smaller scale.**

1. Introduction

From a network operator's point of view, an economical and efficient way to increase the network capacity is attractive. Techniques proposed for increasing the capacity, e.g., additional carriers, sectoring, and microcell deployment, may easily require additional hardware and/or software investments, and therefore increases the operation expenses. Although, many operators are willing to invest more resources in developing their networks, some enhancement methods may require more investments and also more time than expected. Nevertheless, it would be advantageous if the solution for capacity enhancements was fast and flexible.

A base station antenna equipped with electrical downtilt is an attractive choice for an antenna selection, especially in the WCDMA-based UMTS system, where a decrease in the cell interference level is directly reflected into capacity enhancement. An optimum electrical downtilt angle is contributed by many factors: cell range, base station antenna height, and antenna vertical beamwidth. In order to achieve the most excellent performance, the downtilting scheme has to be defined for each site and antenna configuration separately.

Electrical antenna downtilt has been studied in UMTS network in a single 3-sectored site scenario [1]. Downtilt affects clearly the network performance, since rather significant increase in capacity has been observed. The results in [2] suggest that electrical downtilt should be used in an urban environment as a pre-optimisation method. Since these references include only one scenario (i.e., one site spacing, one antenna height, and one antenna vertical beamwidth), it is difficult to define any generalised optimum downtilt angle with the aid of these references. In [3], optimum electrical downtilt angles have been defined using a simple algorithm, but no general definition has been proposed. However, a slight deviation in the optimum electrical downtilt angle has been observed, if the angle has been defined based on the site configuration of a typical urban environment.

The main target of this paper is to realize the impact of different electrical downtilt angles on the network performance, and to find an optimum downtilt angle for different base station site configurations for macrocellular sites in a light urban/suburban environment. The effects of base station antenna height, antenna vertical beamwidth, and site spacing on the optimum electrical downtilt angle has been simulated by using a radio network planning tool. Moreover, both uplink and downlink performances are considered together with an attention to soft handover areas.

2. Electrical antenna downtilt

Electrical downtilt is carried out by adjusting the antenna elements, and hence it slightly changes the antenna radiation characteristics when downtilt angle is changed [4]. Figure 1 illustrates the behaviour of the main, side and back lobes of an electrically downtilted antenna, and shows roughly the changes in the corresponding radiation pattern when downtilt angle is increased.

Since all directions are tilted by the same amount, electrical downtilt reduces other-cell interference very efficiently. This interference reduction in UMTS system can be converted directly into a capacity enhancement. However, also the coverage in the main lobe direction reduces rapidly, which deteriorates the network performance if antennas are downtilted too excessively.

Based on the geometry, an optimum electrical

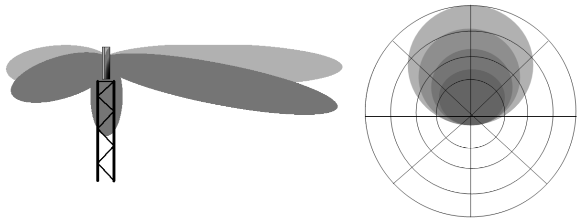

Figure 1: Illustration of electrical antenna downtilt and the corresponding changes in the horizontal radiation pattern.

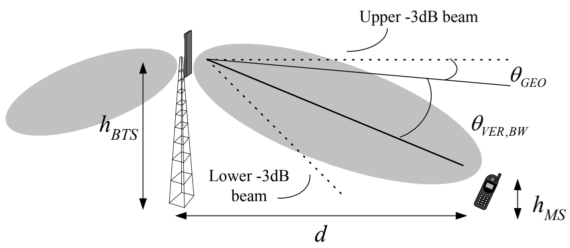

Figure 2: Electrical downtilt scheme and the factors in optimum downtilt angle.

downtilt angle, v_e, is assumed to be a function of the antenna vertical beamwidth factor $\theta_{VER,BW}$ and the geometrical factor θ_{GEO}:

$$v_e = f(\theta_{VER,BW}, \theta_{GEO}). \tag{1}$$

Obviously, the weight of the vertical beamwidth factor is quite high, which can be concluded from geometrical dependencies. If an antenna of a larger vertical beamwidth is utilized, more downtilt is required in order to point the upper -3 dB lobe towards the ground (Figure 2).

Geometrical factor depends at least on the base station antenna height and the site spacing. Higher antenna position as well as smaller site spacing yield for a larger downtilt angle. The geometrical dependence can be defined as in Equation (2):

$$d = \frac{\Delta h}{tan(\theta_{GEO})} \tag{2}$$

where Δh is the height difference between the base station antenna height (h_{BTS}) and the mobile station antenna height (h_{MS}). How d is thereafter selected, depends on the soft handover (SHO) area definitions and required coverage overlapping (indoor coverage thresholds).

In a certain situation, soft handovers give additional gain to the link budget due to macro diversity [5]. If handover areas are widely spread, the signal level differences between soft handover links become larger and the observed gains decrease. The signal field strength near the base station becomes better, if antennas are downtilted and directed more precisely towards the intended serving area (dominance area). Therefore, these sector dominance areas become clearer. Since the coverage overlapping is reduced as a consequence of downtilt, also soft handover areas squeezed and overall soft handover probability decreases.

3. Simulation scenario

Monte-Carlo simulations were utilized in order to verify the performance of UMTS network under different downtilt simulation scenarios. An accurate digital map (including morphological and topographical data of the simulation area as well as the building information in a raster form) was given as an input for the simulator. In the simulation, 19 base station sites with 3-sectored (65° antenna horizontal beamwidth) configuration were located in a regular hexagonal grid. COST-231-Hata propagation model was chosen for the simulations, and an average area correction factor was set to -6.7 dB (light urban/suburban). The used propagation model included also a parameter for modelling diffractions. The user profile consisted only of speech users (12.2kbit/s), which was homogenous. Other general simulation parameters are gathered in Table 1.

Base Station	
Maximum transmit power	43 dBm
Common pilot channel (CPICH)	33 dBm
Other common channels (CCCH)	30 dBm
Synchronisation channel (SCH)	30 dBm
Maximum power per connection	38 dBm
Noise figure	5 dB
Required E_b/N_0	5 dB
Mobile Station	
Maximum transmit power	21 dBm
Dynamic range	70 dBm
Power step size	0.5 dB
Required E_c/N_0	-17 dB
Noise figure	9 dB
Required E_b/N_0	8 dB
Other	
Slow fading standard deviation	8 dB
UL noise rise	6 dB
DL orthogonality	0.6
SHO window	4 dB

Table 1: General simulation parameters.

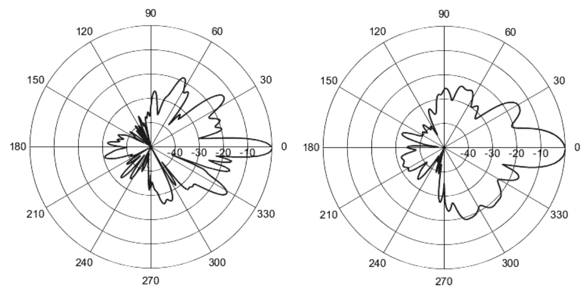

a) b)

Figure 1 : Vertical radiation patterns of antennas used in simulations a) 6° (18 dBi gain) and b) 12° (15 dBi gain).

The selected antenna vertical beamwidths were 6° and 12° (Figure 1). The base station antenna heights (25 m, 35 m, and 45 m) were selected based on practical considerations for a suburban macrocellular network. The site spacings (1.5 km, 2.0 km, and 2.5 km) were chosen in order to realize the effects of antenna downtilt in a noise sensitive network (1.5 km site spacing) and in a coverage sensitive network (2.5 km site spacing).

4. Simulation results

The simulation results are shown with low and high load scenarios. Networks were loaded differently in order to realize the impact of cell-breathing. Different antenna downtilt angles are compared by means of provided service probability and the corresponding downlink normalized load. Antenna downtilt angle is shown respect to service probability and to downlink (DL) normalized load, which is the ratio of the average traffic channel (TCH) transmit power and the maximum power allocated for traffic channel (Equation 3).

$$DL\_load = \frac{average\_TCH\_power}{max\_TCH\_power} \quad (3)$$

An optimum downtilt angle is defined from service probability. First, the maximum service probabilities from the low (grey line) and high (black line) load scenarios are collected. Secondly, the lower and upper boundaries are searched. The lower boundary is the point where the service probability of high loaded scenario has decreased to 0.5% of its maximum value. This lower boundary describes the point where interference level is low enough. The low load scenario does not affect the lower boundary because interferences are at low level. Coverage limitations define the upper boundary, and it is searched from both the low and high load scenarios. The upper boundary is the point where the service probability at the low load scenarios has dropped 1% or at high load scenarios 0.5%. An optimum tilt angle is then assumed to exist between these boundaries, and reported optimum angle is the mean value of the boundary points.

4.1. 6° vertical beamwidth

In Figure 4, the results from the simulations with antenna of 6° vertical beamwidth, 25 m antenna height, and 1.5 km site spacing are presented. In the low load scenario, the interference level in the network remains relatively low; this is indicated with a low downlink load and almost maximum service probability. After a certain downtilt angle, the network coverage becomes the limiting factor in performance, and service probability start to decrease. In the high load and non-tilted scenario, high other-cell interference level is deteriorating the network performance. Moreover, the downlink load achieves relatively high value (0.7). However, increasing the downtilt angle, clearly improves the network performance. Again, at higher downtilt angles, the coverage limits the performance. In the high load scenario, downlink load is gradually decreasing towards higher downtilt angles, and the system performance decreases due to the uplink coverage limitation. Thus, cell-breathing affects the achieved service probability, which can be observed as a cap in the service probability curves between the low load and the high load scenarios.

Increasing the site spacing into 2.5 km does not affect the performance in the low load scenario (Figure 5); the service probability is only slightly lower due to coverage restrictions. Nevertheless, the service probability starts to decrease a bit earlier than with the smaller site spacing. Also, in the non-tilted high loaded scenario, increase in site spacing does not affect the service probability. However, it slightly decreases the downlink load due to smaller interference level. On the other hand, after downtilting the antennas, the service probability is not rising as fast as in previous scenario. Due to coverage and interference limitations, only 0.92 service probability is reached at maximum. The cell-breathing can also be observed more clearly at higher downtilt angles.

In Figure 6, the effect of higher antenna position, and hence larger coverage overlapping, is illustrated with topology of site spacing is 1.5 km and antenna height 45 m. The low load scenario acts similarly to the previous network topologies, and the service probability decreases after an excessively large downtilt angle. On the contrary, in the high load scenario, the effect of higher other-cell interference is more obvious. Before tilting, the service probability is almost as low as 0.6 because of high interference level, which is also indicated with high downlink load. After downtilting, the service probability increases rapidly and reaches almost the maximum achievable. Moreover, at the highest performance, the downlink load remains lower than in the previous simulation scenarios. This indicates better network performance for higher antenna positions with appropriate downtilt angle. Furthermore, the cell-breathing is not seen as strongly as in previous topologies.

In Figure 7 (higher antenna positions and a larger

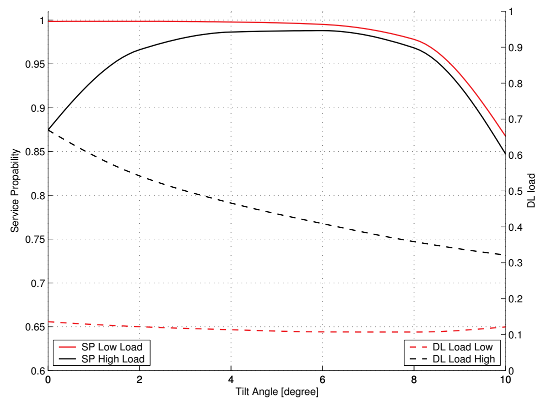

Figure 4: Service probability and downlink load as a function of tilt angle. Antenna vertical beamwidth 6°, antenna height 25 m, and site spacing 1.5 km.

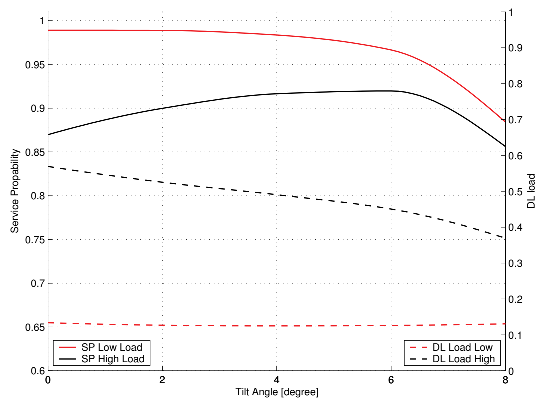

Figure 5: Service probability and downlink load as a function of tilt angle. Antenna vertical beamwidth 6°, antenna heights 25 m, and site spacing 2.5 km.

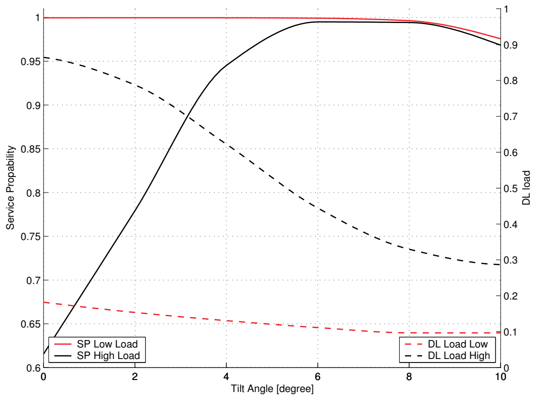

Figure 6: Service probability and downlink load as a function of downtilt angle. Antenna vertical beamwidth 12°, antenna height 25 m, and site spacing 1.5 km.

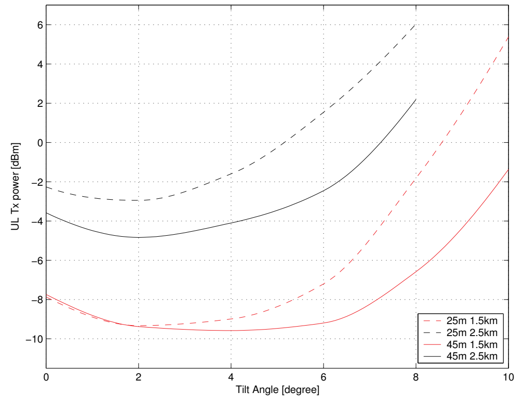

Figure 8: Uplink average transmit powers (high load scenario) as a function of downtilt angle. Antenna vertical beamwidth 6°.

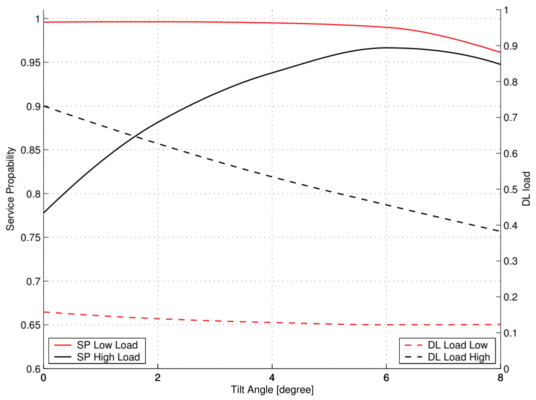

Figure 7: Service probability and downlink load as a function of tilt angle. Antenna vertical beamwidth 6°, antenna height 45 m, and site spacing 1.5 km.

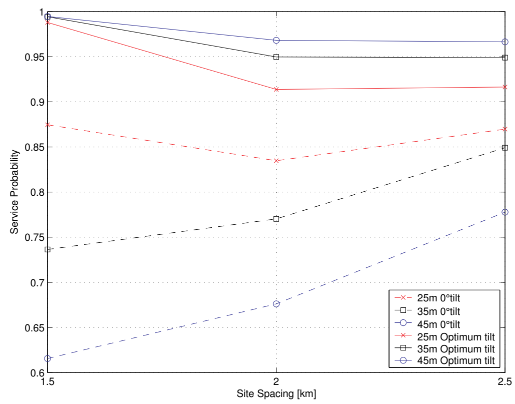

Figure 9: Service probabilities of high loaded networks as a function of site spacing. Antenna vertical beamwidth 6°.

site spacing), the low load scenario behaves expectedly, since the coverage restricts the performance at higher downtilt angles. In the high load scenario, the larger site spacing restricts the coverage and the maximum service probability is not reached. Still, the network performance is better compared to the lower antenna topology.

In Figure 8, the behaviour of the uplink average transmit powers of the preceding high loaded simulation scenarios are shown. At lower downtilt angles, higher interference demands higher average transmit powers as in downlink direction. However, there is always a local minimum in the uplink transmit (Tx) power that cannot be observed in the downlink powers. After this local minimum, the average uplink transmit power is rising according to downtilt angle. The lowest uplink average transmit power level is achieved with 2-4° downtilt angles. After this particular range, the powers begin to increase exponentially. Thus, increasing the downtilt angle changes the network state from downlink limited (indicated with higher downlink load) to uplink limited configuration. Naturally, the average uplink transmit power level is rising also as a function of antenna height and site spacing.

Figure 9 shows the effects of downtilt more comprehensively as a function of site spacing. The solid lines correspond to optimum downtilt and dotted lines non-tilted scenarios. The improvement of the network performance due to antenna downtilting is emphasized with smaller site spacings when other-cell interference levels are higher. However, the network performance equalizes after the site spacing increases, i.e., when the network performance becomes more coverage-limited. Interestingly, higher antenna position results better system performance in the optimum downtilt scenario. This supports the conclusion that the capacity, achieved by downtilting the antennas, is larger when the antennas are installed higher. In optimum downtilt scenarios, the site spacing and antenna height does not affect as dramatically the service probability as in non-tilted scenarios. Thus, the use of antenna downtilt also stabilizes network behaviour.

4.2. 12° vertical beamwidth

Exactly the same simulation topologies were carried out with the antenna of 12° vertical beamwidth. In Figure 10, results of network topology of 1.5 km site spacing and 25 m antenna height are shown. Due to

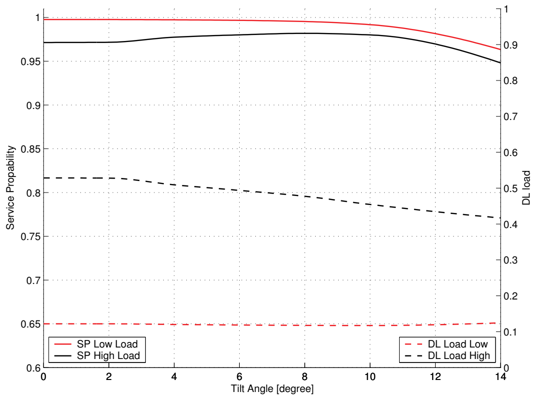

Figure 10: Service probability and downlink load as a function of downtilt angle. Antenna vertical beamwidth 12°, antenna height 25 m, and site spacing 1.5 km.

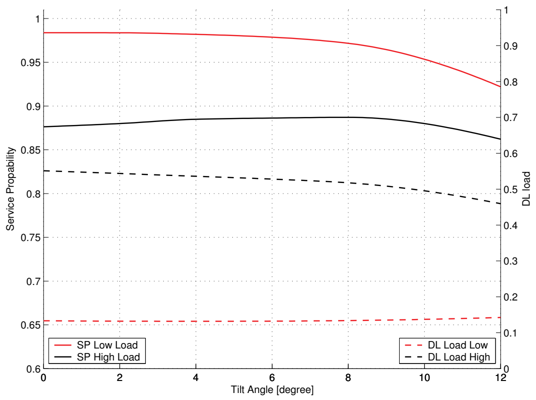

Figure 11: Service probability and downlink load as a function of downtilt angle. Antenna vertical beamwidth 12°, antenna height 25 m, and site spacing 2.5 km.

wider antenna vertical beamwidth and smaller gain, interference is not at high level compared to antenna configuration of 6° antennas. Thus, with high load, the service probability of non-tilted scenario is almost the maximum achievable. Since the interference is not dominating, the benefit of downtilting is only a small. Altogether, the trend of the system performance is the same, but the changes (range from 0 to 10°) are not that spectacular. However, the low load scenarios are almost the same in sense that at lower downtilt angle the service probability remains nearly at the maximum, but at higher downtilt angles, the coverage restricts the performance. The changes in the downlink load are also negligible compared to 6° antenna configuration.

After increasing the site spacing, the network performance of the non-tilted scenario is decreasing due to the coverage limitation (Figure 11). Since the network is rather in coverage-limited than in interference-limited state, the service probability can only be slightly enhanced towards the optimum downtilt angle. Altogether, the changes in the service probability and in the downlink load are very small compared to the simulations of 6° antenna configuration. The optimum downtilt angles are also obviously higher in the wider vertical beamwidth simulations.

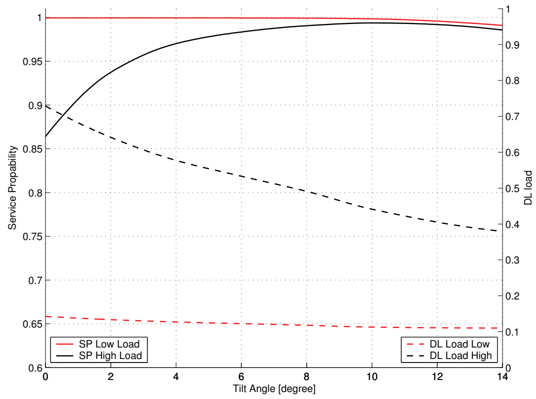

Figure 12: Service probability and downlink load as a function of downtilt angle. Antenna vertical beamwidth 12°, antenna height 45 m, and site spacing 1.5 km.

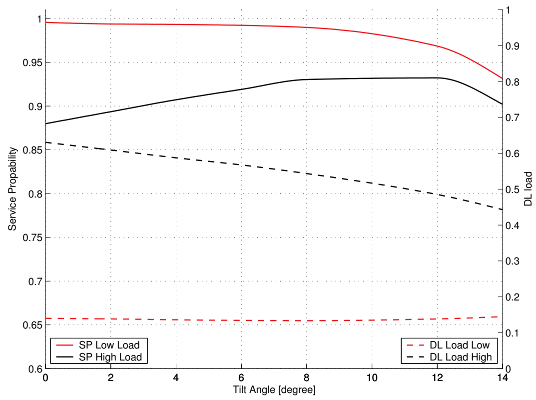

Figure 13: Service probability and downlink load as a function of downtilt angle. Antenna vertical beamwidth 12°, antenna height 45 m, and site spacing 2.5 km.

Figure 12 shows the results with 45 m antenna height. Clearly, other-cell interference is higher, and thus tilting affects more the system performance. The optimum downtilt angle increases, and the changes in the downlink load are also more significant.

In Figure 13 with the topology of 2.5 km site spacing and 45 m antenna height, the performance is similar to the smaller site spacing; expect that the coverage limitation emerges as in previous scenarios. In the non-tilted scenario, the performance remains at the same level compared to corresponding 1.5 km topology.

Average uplink transmit powers are shown in Figure 14. The curves of different scenarios act expectedly and similarly as in 6° antenna configuration. The most significant difference is that transmit powers begin to increase not before 4-8° due to wider vertical antenna beamwidth.

Figure 15 shows the comparison between non-tilted scenarios (dashed lines) and optimum downtilt angle scenarios (solid line). Altogether, downtilt improves the network performance but in a smaller scale compared to 6° antenna configuration. This is partly caused by the fact that the network is not as interference-limited with the same site locations due to smaller antenna gain. Moreover, in order to gain from the downtilt,

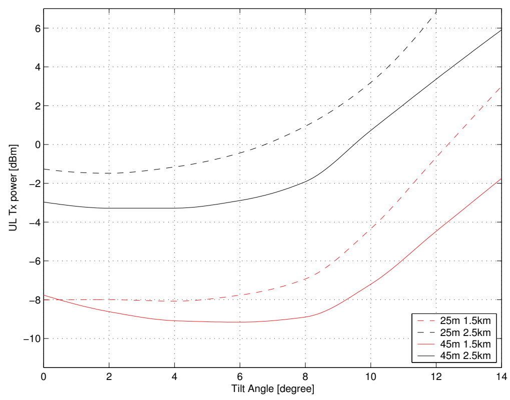

Figure 14 Uplink average transmit powers (high load scenario) as a function of downtilt angle. Antenna vertical beamwidth 12°.

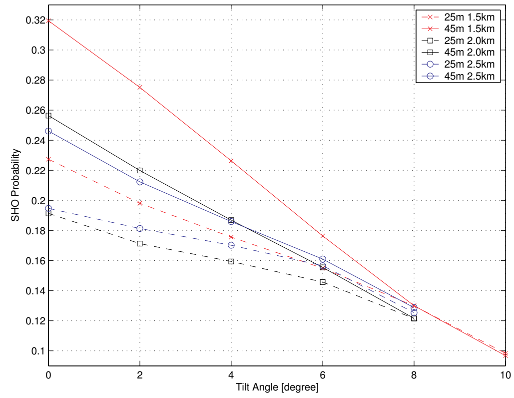

Figure 16: SHO probabilities as a function of downtilt angle. Antenna vertical beamwidth 6°.

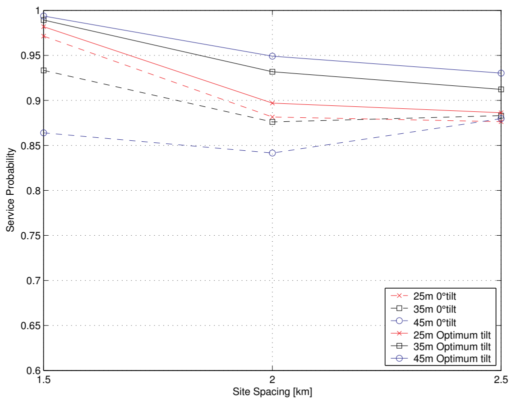

Figure 15: Service probabilities of high loaded networks as a function of site spacing. Antenna vertical beamwidth 12°.

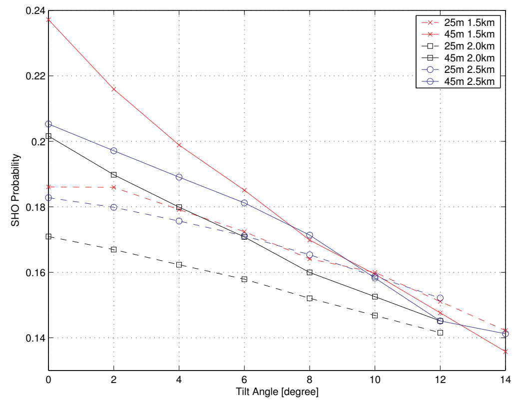

Figure 17: SHO probabilities as a function of downtilt angle. Antenna vertical beamwidth 12°.

interference level has to be larger. As seen from Figure 15, the impact of downtilt is very small; especially with larger site spacing.

4.3. Soft handover probabilities

In Figures 16 and 17, the behaviour of soft handover (SHO) probabilities is presented respect to the antenna downtilt angle of different antenna heights and vertical beamwidths. The probability of soft handover decreases rather linearly as a function of increasing downtilt angle. This is a direct consequence to upper –3dB beam coming closer to the base station, and thus reducing coverage overlapping. The effects are expectedly smaller with the antennas of a wider vertical beamwidth. Intuitively, a higher antenna position creates larger coverage overlapping areas, and hence increases the soft handover probability. Moreover, larger site spacing decreases soft handover probability due to smaller coverage overlapping. With lower downtilt angles, the differences between topologies are emphasized, but towards higher downtilt angles, differences in soft handover probabilities are disappearing.

Figures 18 and 19 show how the soft handover probabilities change according to site spacing in the non-tilted and the optimum downtilt scenarios. Clearly, the changes in the soft handover areas are larger when antennas are not downtilted and if higher antenna positions are used. However, the site spacing has a smaller impact on the soft handover areas. The soft handover probabilities in the non-tilted scenarios are larger with antennas of narrower vertical beamwidth, since the coverage overlapping is larger (higher antenna gain). Nevertheless, the soft handover probabilities in the optimum downtilt scenario are about the same (between 0.15-0.18) regardless of the antenna vertical beamwidth.

5. Discussion and conclusions

In this paper, the impact of the base station electrical antenna downtilt in 3-sectored sites on UMTS network performance has been studied. An optimum downtilt angle was found in all simulated network topologies. The antenna vertical beamwidth has clearly the greatest impact on the optimum downtilt angle, which was expected according to the geometrical analysis. The optimum downtilt angles with antennas of 6° vertical beamwidth were between 4-7°, whereas the corresponding values with antenna of 12° vertical beamwidth were between 5.5-10°. Although, the optimum downtilt angles are given as fixed values, reasonable network performance can be achieved

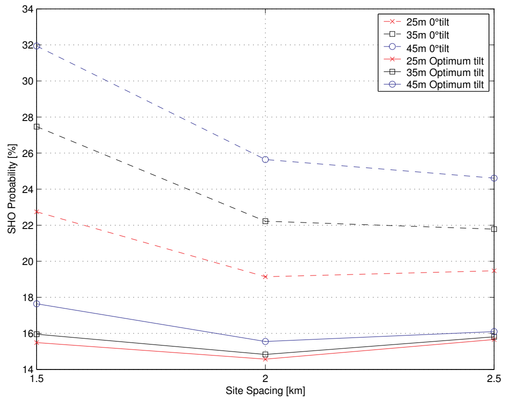

Figure 18: SHO probabilities as a function of site spacing of the optimum downtilt and non-tilted scenarios. Antenna vertical beamwidth 6°.

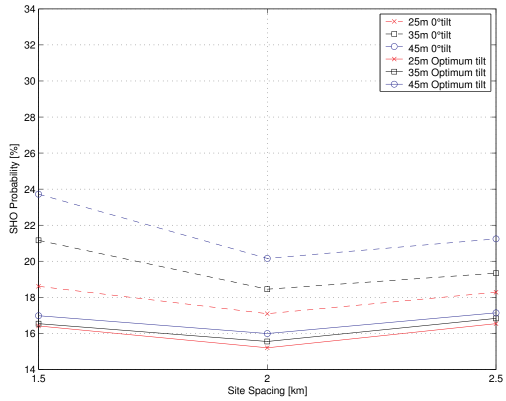

Figure 19: SHO probabilities as a function of site spacing of the optimum downtilt and non-tilted scenarios. Antenna vertical beamwidth 12°.

Site spacing	*1.5 km*		*2.0 km*		*2.5 km*	
Antenna vertical beamwidth/height	6°	12°	6°	12°	6°	12°
25 m	5.3°	7.5°	4.3°	5.8°	4.2°	5.5°
35 m	6.0°	9.0°	5.8°	8.0°	5.4°	7.8°
45 m	7.0°	10.0°	6.3°	9.3°	6.0°	8.3°

Table 2: Optimum downtilt angles of all simulation scenarios.

within a range near the optimum downtilt angle. The allowable range from optimum angle varied: it was larger with wider antenna vertical beamwidth and smaller with higher antenna position.

Table 2 gathers the optimum downtilt angles of all simulation scenarios. Clearly, different antenna height changes the optimum downtilt angle almost in all scenarios. However, an increase of site spacing does not always decrease the optimum downtilt angle as could have been expected according to geometrical analysis.

Compared to the antenna vertical beamwidth, the base station antenna height and site spacing affect in a smaller scale on the optimum downtilt angle. As a consequence of a higher antenna position, other-cell interference raises causing degradation in the network performance. The network performance can be maintained (or even improved) if antennas are downtilted. Thus, the effect of downtilting should be emphasized in case of higher antenna positions. Site spacing affects also expectedly the optimal downtilting angles, although the behaviour is not linear.

The network behaves differently if antennas are downtilted. Especially, in the non-tilt scenarios with higher antenna positions and smaller site spacings, the downlink load is higher due to high other-cell interference, and moreover it has a tendency to decrease when the antennas are downtilted. On the contrary, uplink transmit powers are increasing after a certain downtilt angle, and towards higher downtilt angles, the network becomes strongly uplink coverage limited.

The soft handover probability is decreasing almost linearly with respect to downtilt angle. If site locations are kept fixed, narrower antenna vertical beamwidth (higher antenna gain) results larger soft handover areas than wider antenna vertical beamwidth. However, in the optimum downtilt scenarios of different antenna vertical beamwidths, the soft handover probabilities are almost the equivalent.

6. Acknowledgements

Authors would like to thank European Communications Engineering (ECE) Ltd for helpful comments concerning simulation parameters and simulation environment, Nokia Networks for providing NetAct Planner tool for simulations, FM Kartta for providing a digital map, and the National Technology Agency of Finland for funding the work.

REFERENCES

[1] I. Forkel, A. Kemper, R. Pabst, R. Hermans, *The Effect of Electrical and Mechanical Antenna Down-Tilting in UMTS Networks*, The Third International Conference on 3G Mobile Communication Technologies, 2002.

[2] Jaana Laiho-Steffens, Achim Wacker, Pauli Aikio, *The Impact of the Radio Network Planning and Site Configuration on the WCDMA Network Capacity and Quality of Service*, IEEE 51st Vehicular Technology Conference, vol. 2, 2000.

[3] A. Wacker, K. Sipilä, A. Kuurne, *Automated and Remotely Optimization of Antenna Subsystem Based on Radio Network Performance*, The 5th International Symposium on Wireless Personal Multimedia Communications, vol. 2, 2002.

[4] William C. Y. Lee, *Mobile Communications Engineering*, McGraw-Hill, 1998.

[5] Jaana Laiho, Achim Wacker, Tomáš Novosad, *Radio Network Planning and Optimisation for UMTS*, John Wiley & Sons Ltd, 2002.